Science of the Total Environment 780 (2021) 146638

Contents lists available at ScienceDirect

Science of the Total Environment

journal homepage: www.elsevier.com/locate/scitotenv

# Shrub changes with proximity to anthropogenic disturbance in boreal wetlands determined using bi-temporal airborne lidar in the Oil Sands Region, Alberta Canada

L. Chasmer [a,*], E. Moura Lima [b], C. Mahoney [c], C. Hopkinson [a], J. Montgomery [c], D. Cobbaert [c]

[a] Dept. of Geography and Environment, University of Lethbridge, Lethbridge, AB, Canada
[b] Graduate Program in Forest Engineering, Universidade Federal de Santa Maria, Camobi, Santa Maria, RS, Brazil
[c] Alberta Environment and Parks, Government of Alberta, Edmonton, AB, Canada

## HIGHLIGHTS

- Linear disturbances have significant, multi-faceted impacts on boreal wetlands.
- Wetlands impacted by disturbance, enhancing shrubs in bogs.
- Greatest anthropogenic disturbance occurs in fens.
- Lidar transects are a low-cost sampling strategy for monitoring wetland change.

## GRAPHICAL ABSTRACT

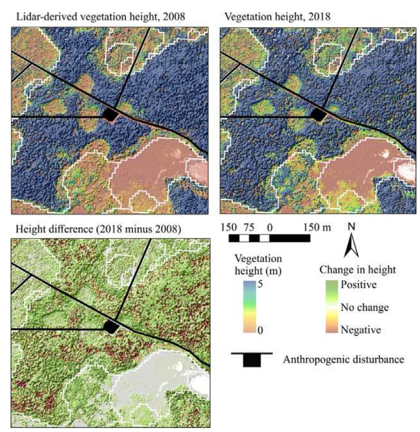


## ARTICLE INFO

*Article history:*
Received 27 November 2020
Received in revised form 17 March 2021
Accepted 17 March 2021
Available online 21 March 2021

Editor: Jay Gan

*Keywords:*
Boreal
Wetland change
Anthropogenic disturbance
Remote sensing
Wetland management

## ABSTRACT

In this study, we used bi-temporal airborne lidar data to compare changes in vegetation height proximal to anthropogenic disturbances in the Oil Sands Region of Alberta, Canada. We hypothesize that relatively low-impact disturbances such as seismic lines will increase the fragmentation of wetlands, resulting in shrub growth. Bi-temporal lidar data collected circa 2008 and 2018 were used to identify correspondence between the density of anthropogenic disturbances, wetland shape complexity and changes in vegetation height within >1800 wetlands near Fort McKay, Alberta, Canada. We found that up to 50% of wetlands were disturbed by anthropogenic disturbance in some parts of the region, with the highest proportional disturbance occurring within fens. Areas of dense anthropogenic disturbance in bogs resulted in increased growth and expansion of shrubs, while we found the opposite to occur in fens and swamps during the 10-year period. Up to 30% of bogs had increased shrubification, while shrub changes in fens and swamps varied depending on density of disturbance and did not necessarily correspond with shrub growth. As wetland shapes became increasingly elongated, the prevalence of shrubs declined between the two time periods, which may be associated with hydrological drivers (e.g. elongated may indicate surface and ground-water discharge influences). The results of this study indicate that linear disturbances such as seismic lines, considered to have relatively minimal impacts on ecosystems, can impact proximal wetland shape, fragmentation and vegetation community changes, especially in bogs.



* Corresponding author.
*E-mail address:* laura.chasmer@uleth.ca (L. Chasmer).

https://doi.org/10.1016/j.scitotenv.2021.146638
0048-9697/

## 1. Introduction

The Boreal Plain ecozone of western and central Canada contains large, heterogeneous areas of boreal wetland and forest complexes spanning approximately 650,000 $km^2$ from north-central British Columbia to southern Manitoba. In central and eastern Alberta, these complex ecosystems are under significant human development pressures due to petroleum exploration, in situ facilities and mining operations, forestry, agriculture and infrastructure operations (Devito et al., 2012; Abib et al., 2019). The Oil Sands Region (OSR) of Alberta encompasses 142,200 $km^2$ area and is underlain by >160 billion barrels of oil, making it the world's third largest oil reserve (Alberta Energy Regulator, 2019). These broad disturbances result in a loss of ecosystems and often dense fragmentation of the landscape (ABMI Human Footprint Inventory, 2019 ABM).

Wetland losses and alterations from oil sands development (or any widespread anthropogenic disturbance) have potentially significant, yet poorly understood implications for ecosystem services (Rooney et al., 2012), especially as these wetlands are further impacted by climate change and fire/insect disturbances (Flannigan et al., 2015; Jiang et al., 2015; Thompson et al., 2017). While air temperature in northern regions is predicted to increase along with precipitation and evaporative fluxes (IPCC, 2014; Ireson et al., 2015), it is not clear whether ecosystems will maintain their current moisture and hydrological characteristics or become drier (e.g. Mwale et al., 2009). Many wetland ecosystems in the OSR are increasingly sensitive to small changes in water balance, which threatens their long-term maintenance (Hokanson et al., 2019; Hokanson et al., 2020). Disturbances that impact energy and water exchanges between the terrestrial biosphere and the atmosphere could create a response towards ecosystem change (Petrone et al., 2007; Petrone et al., 2015), which ultimately impacts the ecosystem services these wetlands provide to local communities (Chasmer et al., 2020a).

The literature on the impacts of petroleum exploration and mining on boreal wetland ecosystems provides important context for the current research: A) Hydrology: The movement and availability of water is identified by Ketcheson et al. (2016) as the most important process required for the maintenance of wetlands and regulation of their function. The position of wetlands with respect to terrain relief impacts their frequency and duration of inundation or saturation, while their landscape connections can play a key role in maintaining adjacent ecosystems, such as upland forests during dry periods (Devito et al., 2005; Smerdon et al., 2008; Devito et al., 2012; Chasmer et al., 2018; Hokanson et al., 2019). B) Vegetation Composition and Structure: Dabros et al. (2018) suggest that while seismic lines are becoming narrower and less impactful to ecosystems, their impacts to adjacent, proximal ecosystems are not well understood. Vegetation species can be impacted for up to 50 years following seismic line and well pad disturbance (Revel et al., 1984; Finnegan et al., 2018). Groot et al. (1997) also suggest that alterations to vegetation structure within seismic lines will increase evapotranspiration rates, causing greater overall surface drying. C) Soil Structures and Terrain: Compaction due to heavy mulching machinery also alters local topographic variability by artificially reducing elevation (Stevenson et al., 2019), depth to water table (Lovitt et al., 2018), and soil micro-climatology when mulch is left on the surface (Lee and Boutin, 2006; van Rensen et al., 2015). Successional processes associated with eventual humification of the catotelm caused by aeration of the upper peat layers with changes in energy balance and evapotranspiration reduces upwelling of nutrient-rich water due to changes in hydraulic conductivity (Nwaishi et al., 2015). This increases catotelm thickness, thereby isolating the acrotelm from groundwater, resulting in nutrient-poor conditions and ombrotrophy.

In situ observations of the ecological effects of disturbance on boreal ecosystems described above provide a mechanistic understanding of hydrological, mechanical, and nutrient drivers of floristic and structural/productivity variations. Field-based observations often use chronosequence or space-for-time experimental approaches (e.g. Hopkinson et al., 2016a, 2016b; Walker et al., 2020), however, because of the extent of the OSR and the relative remoteness of many wetland and forest ecosystems (typically without road access; Chasmer et al., 2020b), field-based methods can be impractical to implement across broad areas and over long time periods. Remote sensing provides an additional means for acquiring information on vegetation structures and species characteristics, which can be examined across broad regions and in some cases, over longer periods of study, beyond typical funding initiatives. Changes in overall wetland vegetation canopy height attributes through time may be considered a proxy for the cumulative environmental drivers that alter wetland and ecotonal vegetation composition and productivity (reviewed in Waddington et al., 2015). It is also important to consider the proportion of wetlands that are experiencing vegetation changes that exceed naturally occurring successional processes and may indicate sensitivity to changing environmental conditions.

Here we used a novel bi-temporal lidar radial transect sampling approach to better understand whether or not changes in shrub and short stature trees occur in wetlands with varying density of anthropogenic disturbances in the OSR over a ~ 10-year period. Lidar is used as a "lots of plots" method (e.g. Wulder et al., 2012) where every cubic meter along each ~1 km wide × ~110 km transect represents a structural and volumetric measurement of vegetation height, foliage cover and ground surface elevation, and change through time. The objectives of this study were to: a) quantify the proportion of wetland classes that have been impacted by anthropogenic disturbances; b) determine if wetland shapes are more complex in areas of high anthropogenic disturbances; and c) determine if there is a relationship between the density of anthropogenic disturbances and change in vegetation height in wetland classes. The implications of human disturbances on wetlands will be examined over hundreds of wetlands using bi-temporal lidar-derived vegetation height change as a proxy of cumulative impact of the underlying local environmental influences and feedbacks that anthropogenic disturbances have on the surrounding proximal wetland ecosystem.

## 2. Material and methods

### 2.1. Study area

The study was located in the mineable oil sands area of northeastern Alberta, Canada (Fig. 1a, inset). The mean annual air temperature is approximately 1 °C, with mean daily temperatures ranging from −17 °C in January to 17 °C in July; average annual precipitation is approximately 420 mm (ECCC, 2019). Prolonged wet and dry periods spanning years can result in vegetation mortality and growth within boreal wetlands and peatlands. Cumulative water year (October to September) Environment Canada precipitation data from nearby Fort McMurray (~60 km) for the 1990–2019 period indicates a wet period from 1991 to 1997, prolonged drought from 1998 to 2002, and relatively stable below 30-year average cumulative water year precipitation from 2004 to 2019, inclusive of the period of study. The surficial geology is composed by fine to coarse textured glaciolacustrine sediments (Fenton et al., 2013; Atkinson et al., 2014; MacCormack et al., 2015) overlain by a deep layer of peat >0.4 m within peatlands. The landscape comprises a mosaic of upland forests, wetlands, and few lakes, where approximately 45% of the surface area is wetland. Of this, 64% are peatlands, 25% are swamps, 8% are shallow open water and 3% are marshes (Ficken et al., 2019).

### 2.2. Airborne lidar data collection and processing

Data were acquired to understand the proximal impacts of oil sands mining activities, exploration and other natural resources extraction related disturbances such as seismic lines, roads, well pads, and forestry operations on boreal ecosystems. The sampling design was set up to capture the variability in the magnitude of landscape disturbance, ranging from on-lease active mining and exploration to off-lease disturbances (i.e. forestry, linear features, etc.), and minimal disturbance. Bitemporal airborne lidar data collections were used to quantify and map change in wetland shrub and short stature tree height over a period ranging from 8 to 11 years. Historical data circa 2008 were surveyed between June and early September to avoid phenological changes.

Lidar data circa 2008 were acquired using a 1064 nm discrete return scanning airborne lidar, (data licensed to the Government of Alberta). The second survey was completed in August 2018 by the University of Lethbridge along eight swath transects, approximately 1 km wide and about 110 km in length using a Teledyne Optech Inc. (Toronto, Canada) Titan multi-spectral lidar (Hopkinson et al., 2016a, 2016b). Transects were approximately centered on Fort McKay near the centre of surrounding oil sands mining operations and extended up to 55 km in cardinal and ordinal directions. From the collected radial transects, three were selected: Transect 1 (NW to SE), Transect 2 (W to E) and Transect 3 (SW to NE) to avoid the inclusion of recent wildfire disturbances (except a small area burned in 1949) (Fig. 1b).

Circa 2008 data were intersected with the extent of the 2018 data (Fig. 1b). Both were processed to determine height of vegetation and ground surface elevation (described below) using 1064 nm. Spatial extents were clipped to the 2018 transect boundaries and point clouds were processed identically using Terrascan (TerraSolid, Inc. Finland) for quality control. Spurious points were removed, including those identified as below ground (multi-path interactions), high points, and ground classification. Ground classified lidar data from circa 2008 and 2018 were rasterized to create a digital elevation model (DEM). Vegetation height at 2 m cell resolution was estimated from the 95th percentile height (P95) of all points lying above the DEM ground surface using LasTools (RapidLasso, GmbH, Germany). P95 was selected over alternate vegetation height measures because it has demonstrated correlation with field verified vegetation heights in Canada's boreal forest (Mahoney et al., 2018). To determine changes in vegetation height over the ~10-year period, P95 vegetation heights from 2008 were subtracted from P95 vegetation heights from 2018 for each individual cell.

### 2.3. Supplementary geospatial data

The Human Footprint Inventory (HFI) circa 2017 (ABMI Human Footprint Inventory, 2019) was used as a spatial metric to quantify the extent of different anthropogenic disturbances from satellite imagery. In addition, we used the Predictive Landcover 3.0 product of the Advanced Landcover Prediction and Habitat (ALPHA) series to identify wetland classes (ABMI, 2019). The Landcover product used data from Sentinel-1 and Sentinel-2 (10 m spatial resolution) within a convolutional neural network deep learning approach trained and validated using reference data from over 800 interpreted 3 km × 7 km photo plots (ABMI, 2016) located across Alberta. The product classified approximately 77% of the land surface of Alberta, identifying seven classes: bog, fen, marsh, swamp, open water, upland and a general 'wetland' class. The product is reported with relatively high accuracy where peatlands and mineral wetlands were assessed with 87% and 69% overall accuracies, respectively (DeLancey et al., 2019).

### 2.4. Determining wetland complexity associated with disturbance

To determine the indirect impacts of human disturbance on wetlands, we removed all wetland areas that intersect directly with disturbance, based on the HFI. All other wetland areas adjacent to the disturbance (but not disturbed) were included in the analysis. The frequency of HFI within each wetland class was determined by binning wetland areas into 5 km segments, illustrated in Fig. 1b and calculating proportional area coverage within wetlands. In addition, an index of complexity was determined at the class level within each 5 km segment. Changes in vegetation height was determined by sampling random points distributed >5 m from each adjacent point, divided into wetland classes, to reduce the potential for spatial autocorrelation within wetlands. The variation between randomly extracted vegetation heights was used to calculate height variability (standard deviation within each wetland). Change in area coverage between 2008 and 2018 was compared within individual wetlands separated into classes. These were compared with proportional HFI coverage, wetland length, area, and length:area ratio.

The index of complexity of wetlands, which may be associated with the frequency and area extent of human disturbances, was determined per wetland class within 5 km segments. The complexity of wetlands was determined using 'landscapemetrics' R package (Hesselbarth et al., 2019). Complexity is a measure of the mean shape index, such that those patches that approach a circular shape are equal to 1. The mean shape index increases to greater than 1 as the wetland patch becomes more complex. Therefore, we hypothesize that wetlands that have been directly disturbed by seismic lines will be partitioned into smaller component parts and will be less likely to resemble circular shapes, thereby increasing their 'complexity index'.

### 2.5. Characterizing wetland vegetation height differences

To quantify wetland vegetation height differences between 2008 and 2018, we examined changes in shrub and short tree vegetation in all disturbed and undisturbed wetlands along transects. Shrub and short tree vegetation (>0.5 m and <3 m) was identified and classified within wetlands in both 2008 and 2018 lidar data (ESRD, 2015). In addition, the impacts of the density of proximal disturbance (or lack thereof) on wetlands were determined to a buffer distance of 500 m from wetland edges. To determine the proportional area of wetlands that experienced increased shrubification, all grid cells within wetlands with a change in vegetation height ≥ 1 m between 2008 and 2018 were identified and compared. Coefficient of determination was used to compare wetland characteristics (e.g. complexity, area, length, length:area ratio) with percent density of HFI, wetland area change, and vegetation change over the 10-year period. A Kruskal-Wallis chi-squared test was used to examine shrub proportional area change in wetlands with increasing proportion of HFI using alpha of 0.01. A Bonferroni correction was applied to determine if significant differences exist between vegetation changes within HFI proportional classes and no change. Geospatial and statistical analyses were performed in R, ArcGIS (ESRI, CA) and Systat (Systat Software, San Jose, CA).

## 3. Results

### 3.1. Proportion of wetland classes impacted by anthropogenic disturbances

Within the lidar sampling transects, 984 peatlands (246 bogs and 738 fens), 802 swamps, 194 marshes, and 156 open water bodies were identified from the ALPHA classification (ABMI, 2019). The distribution of wetlands along lidar transects is highly variable: bogs and fens represent approximately 34, 18 and 19% for transects 1, 2 and 3, respectively. Swamps are less common, representing between 4% and 9% of the total area, where marsh and open water each represent approximately 1% of the total area (Fig. 2).

The highest proportion of HFI disturbance was found in Transects 1 and 2, where 20.5 and 22.3% of anthropogenic disturbance was found in wetlands, while 16.9% of wetland areas were disturbed by anthropogenic disturbance in Transect 3 (Fig. 3). Within each transect, the largest proportion of HFI was consistently found in fens, which accounted for between 3% (Transect 3) and 10% (Transect 1) of total HFI (total = 18.1%), followed by swamp (10.8%), bog (8.4%) and marsh (7.5%). The distribution of the proportion of HFI within 5 km increments per

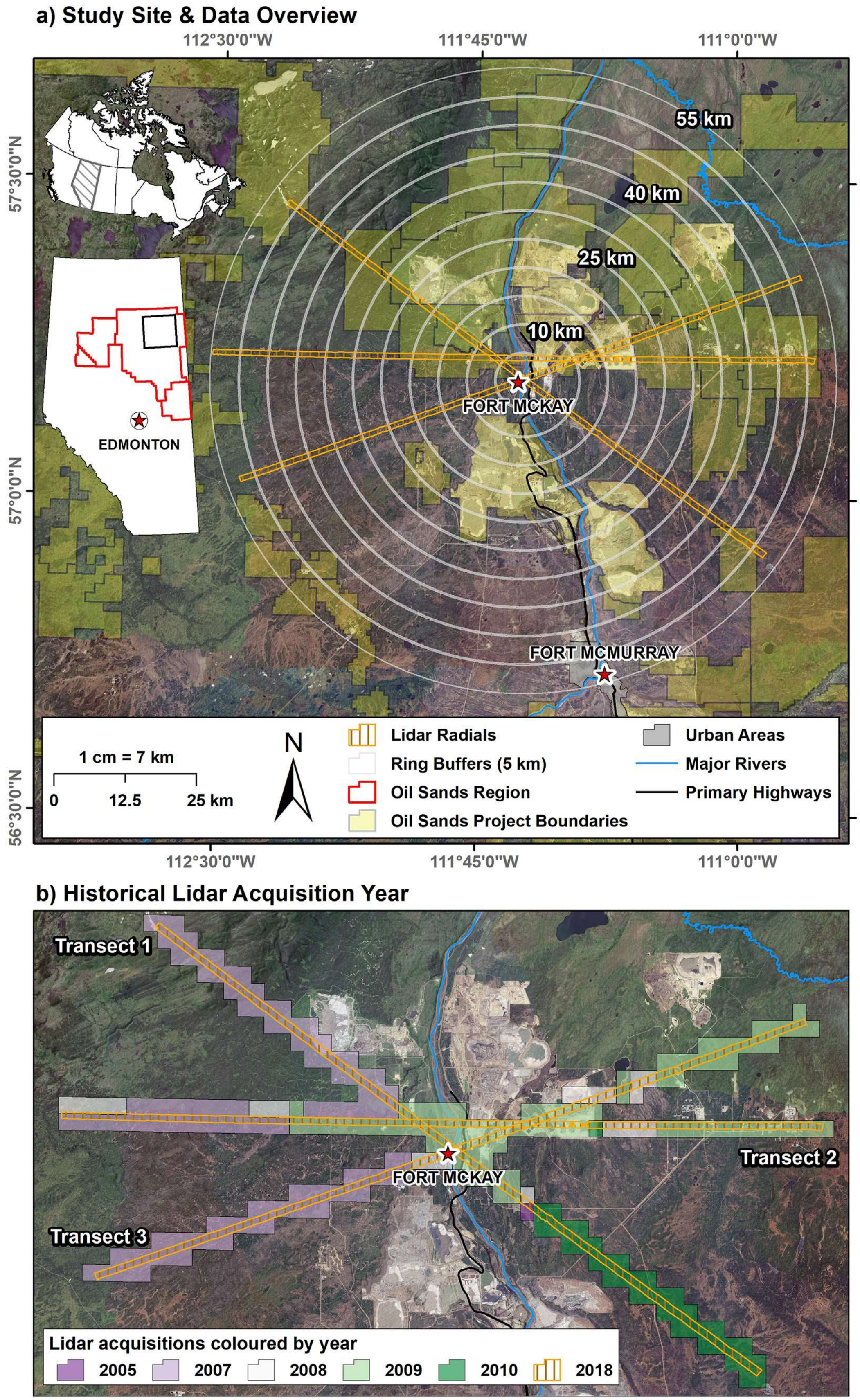


**Fig. 1.** Location of radial lidar transects centered on Fort McKay in the Athabasca Oil Sands Region of Alberta, Canada (inset maps). a) Three lidar transects (approximately 100 to 110 km in length) are illustrated with 5 km radial buffers 'segments' overlaid. Potential high disturbance areas are noted by the 'Oil Sands Project Boundaries' which denotes project lease boundaries where oil sands activities are permitted, whether it be active mining or exploration only; b) The year of provincial lidar data acquisitions along 2018 lidar data collection transects used in this study.

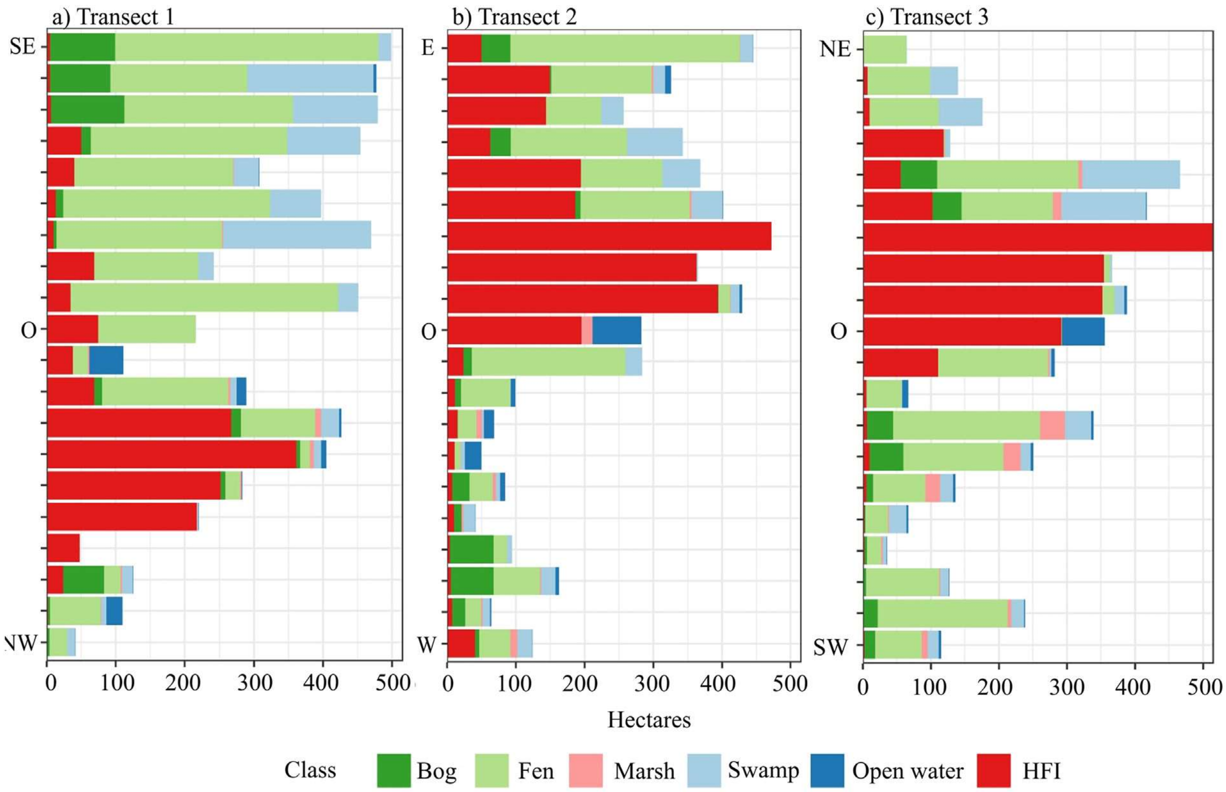


**Fig. 2.** Cumulative areas of anthropogenic disturbance (HFI) and wetland class in hectares divided into 5 km segments from transect centres (O) to their respective edges within lidar transects 1–3.

wetland along lidar transects is illustrated in Fig. 3, where proportion of total HFI found within wetlands is divided into wetland classes. The proportion of wetland area disturbed ranges between less than 1 to ~50% (Transect 1), 22% (Transect 2) and less ~9% (Transect 3).

### *3.2. Comparing wetland shape complexity variations with density of HFI*

Wetland interception via HFI, especially seismic lines, may enhance the complexity of wetland shapes. Fig. 4 illustrates variations in wetland complexity combined for all wetlands and proportional density of total HFI found within 5 km lidar transect segments from east to west. The positive relationship between wetland complexity and density of HFI occurs along the full extent of transect 3 (Fig. 4c). Shape complexity and density of HFI do not correspond along transects 1 or 2, especially in areas of high disturbance west of the centre of transects. HFI complexity illustrated in the third panel of Fig. 4 corresponds with the density of HFI: as more HFI intersect within wetlands, the length of HFI edges increases. The relationship between HFI density, wetland complexity and HFI complexity is significant within transect 3 (Fig. 4c), however, may be skewed by the proportional coverage of open pit mining operations in Transect 1, which cover between 80 and 94% of some transect sections.

### *3.3. Relationship between the density of anthropogenic disturbances and change in vegetation height, shrub area*

The relationships between anthropogenic disturbances and shrub/short tree vegetation height changes illustrated in Table 1 are complex. Anthropogenic disturbances do not consistently correspond with increases in vegetation height across all wetland classes and characteristics as we had hypothesized. Increased proportion of HFI corresponds with increased shrubification in bogs ($R = 0.19$; $p = 0.003$), with greater shrub establishment occurring in areas with high proportions of linear features and well pads (excluding open mining areas) ($R = 0.28$; $p < 0.0001$). However, the area of shrubs within fens and swamps have declined with increasing proportional coverage of HFI over 10 years ($R = -0.16$, $p < 0.0001$; $-0.18$, $p < 0.0001$), respectively. Fens and swamps had strong negative relationship between the ratio of the wetland length to the area (L:A), such that fens and swamps with lower L:A ratio (rounded features) had increased expansion of shrubs ($R = -0.14$, $p < 0.0001$; $-0.21$, $p < 0.0001$), which decreased as these wetlands became more elongated. The strength of this relationship increased in swamp areas that excluded large proportional coverage of open-pit mining. Shrub and tree height increases were also greater in swamps that have lower L:A over the 10-year period. In addition, all wetland classes were characterized by increasing variability of vegetation heights (standard deviation) over the 10-year period in wetlands with lower L:A ratios, while becoming increasingly less variable as wetland shapes became more elongated. This relationship is strongest in swamps and marshes, while bogs and fens exhibit significant ($p < 0.0001$) but less height variability with shape.

The relationship between shrub/short tree changes over time is complicated by the proportional coverage of HFI within wetlands (Fig. 5). Significant differences (alpha $= 0.01$) in shrub area across all HFI proportions occur within bogs ($p$-value $= 0.00035$) and swamps (p-value $= 0.0001$). Shrub area expansion occurs predominantly in wetlands to an approximate density of 20% proportional area disturbance in bog and swamp wetland classes compared with the mean shrub changes in undisturbed wetlands of the same class (indicated by no change or 0). Bogs experienced the greatest increase in shrub area increase between 2008 and 2018, ranging on average from 7 to 14%, extending to ~30% (wetland area expansion of shrubs, stdev $\pm$ 17%). Wetlands containing or proximal to 45% or more area disturbance have reduced proportional area of shrubs, while disturbances covering <10% of wetland and proximal ecosystems were not significantly different from undisturbed wetlands. Marsh wetlands did not demonstrate a dominant trend of shrub

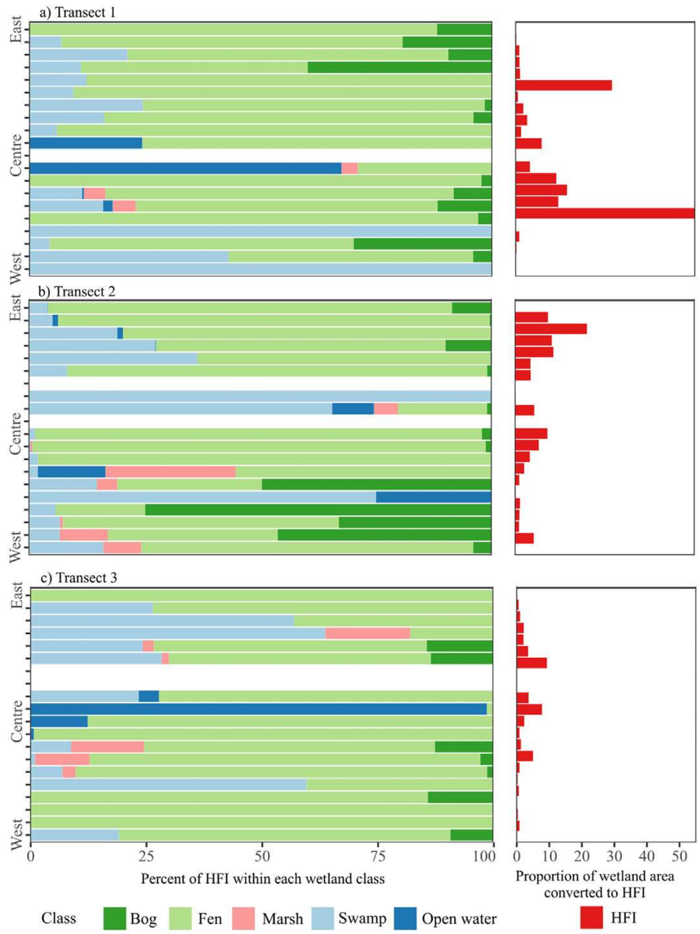


**Fig. 3.** The proportion of total HFI found within wetlands along each lidar transect divided into wetland class (left) and proportion of HFI found within each transect 5 km segment impacting wetlands (right).

succession or mortality from 2008 to 2018 with increased HFI area cover.

The encroachment and decline of shrubs and short stature trees across lidar transects (Fig. 6) is complicated by the proportional density of HFI found within and proximal to wetlands (Table 1), wetland class, and characteristics, and other environmental influences not examined in this paper (e.g. surficial geology, atmospheric deposition) (e.g. Wieder et al., 2019). Fig. 6 illustrates wetland areas that have undergone the most extensive changes in shrub and short tree coverage within wetlands. Rapid increase in vegetation height exceeding 30% of combined wetland area associated with an area of high density seismic lines (~crossing perpendicularly every 40 m to every 100 m) east of open mining areas, and further from mining development along transects 2 and 3. Wetlands found along the south-eastern zone of transect 1 were characterized by vegetation decline. The variability in rates of vegetation change within wetlands over the period of study indicates that a variety of cumulative and proximal environmental drivers influence the sensitivity of wetlands to enhanced change and require further investigation.

## 4. Discussion

### 4.1. Use of lidar for examining bi-temporal changes in wetland vegetation structure

In this study, we demonstrated the utility of bi-temporal airborne lidar data to quantify differences in vegetation height and area coverage as these relate to proportion of anthropogenic disturbance, wetland and HFI characteristics. Airborne lidar was used to measure vegetation height at two dates in time by using the rapid emission and reception of laser pulses and comparing the differences in the vertical distribution of the returns (Lefsky et al., 1999). Lidar-based classification provides an accurate, cost-effective means for characterizing wetland ecosystem structure (Goodale et al., 2007; Montgomery et al., 2019; Chasmer et al., 2020b), and bi-temporal datasets can be used to elucidate changes in vegetation structures over time (e.g. Hopkinson et al., 2008). Based on a review of the literature, Waddington et al. (2015) suggest that positive shrubification feedbacks may be associated with a decline in water table in boreal bogs and poor fens, while other local environmental drivers may increase the height of the water table. Spatial differences in shrub height over time are an indicator of wetland response to one or more stressors. These changes can be monitored using lidar or other remote sensing-based methods and field data collection as proxy indicators of the environmental changes driving shrub/short tree growth or loss.

### 4.2. Major disturbance patterns and influences on vegetation communities, hydrology and energy

HFI is one of the largest disturbance mechanisms in the OSR, with up to 50% of HFI intercepting wetland classes (Fig. 2). The transects surveyed using lidar cover high disturbance areas with up to 25% of the total cumulative proportion of HFI exceeding the average of 15% reported by Ficken et al. (2019). In some areas along the lidar transects, HFI proportion was up to 50% of wetlands within the 5 km segments, while in other segments these were less than 1% (Fig. 2). This provides an opportunity to determine if relationships exist between anthropogenic disturbance and wetland shrub/short tree vegetation changes.

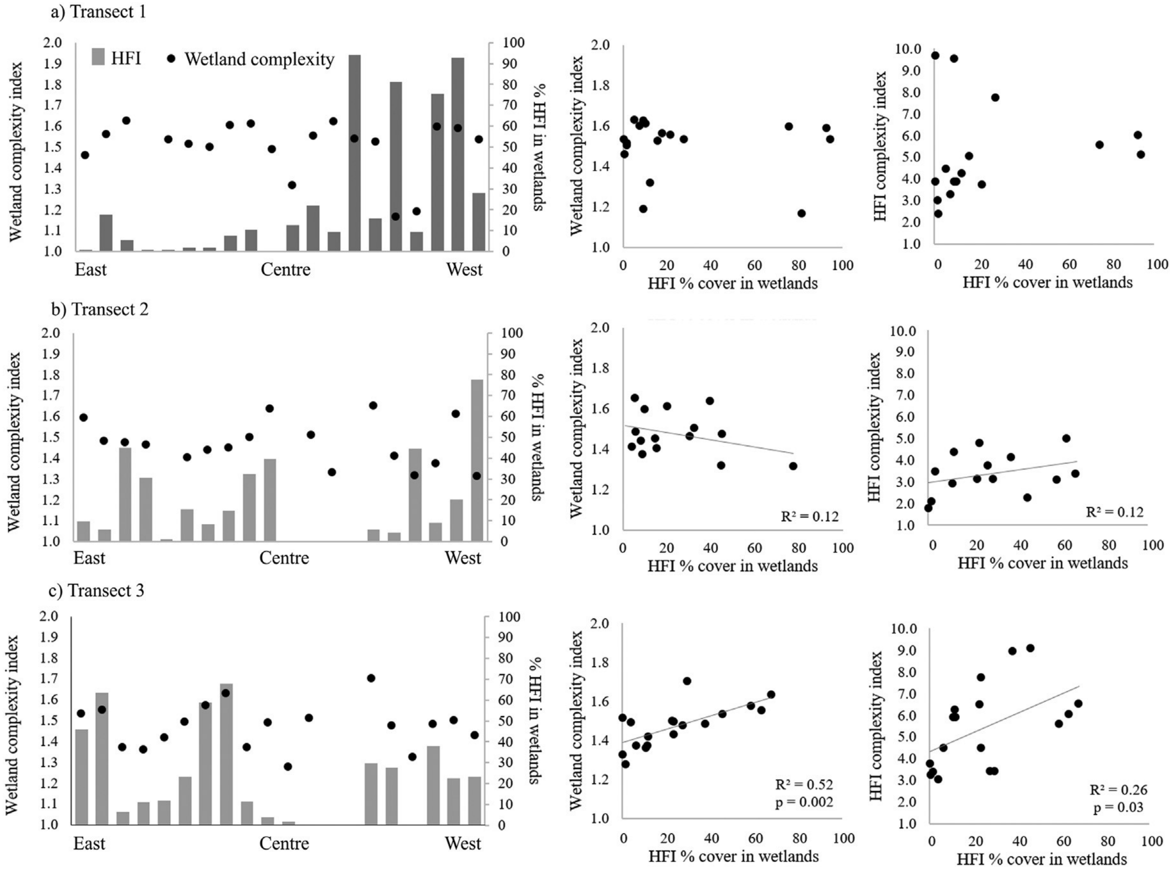


**Fig. 4.** Comparison between wetland complexity index and HFI density (left and centre) and HFI complexity associated with the proportion of total HFI found in wetlands (right) within 5 km segments for transects 1–3 (a–c).

In this study we hypothesized that the fragmentation of wetlands by HFI would increase the complexity of wetland shapes, such that wetlands would be less circular or compact in shape. We hypothesized that the complexity of the wetland shape and proximity to anthropogenic disturbance would alter wetland vegetation species communities and structures, enhancing growth. In another study, Ficken et al. (2019) found that wetlands that were intersected by HFI contained non-obligate wetland plant species, typically found in well-drained forests, while undisturbed wetlands contained a higher proportion of obligate wetland species. Here we found that wetland shape complexity corresponded with increasing proportion of HFI within wetlands ($R^2 = 0.52$, $p = 0.002$) along transect 3 (Fig. 3) but did not significantly correspond across all proportions of HFI along transects 1 and 2. This may indicate that only some disturbances, such as seismic lines, influence wetland shape, whereas other disturbances such as open-pit mining have less influence on wetland shape relative to proportional coverage. Changes in wetland shape may increase the potential for expansion of non-obligate species found by Ficken et al. (2019) and should

**Table 1**
Comparisons between wetland attributes: longest cross section (length, L), area (A), length to area (L:A) where higher numbers refer to increasingly rounded wetlands, and all %HFI, vegetation changes within 500 m of wetlands across all transects, combined. %HFI are also examined for wetlands where HFI includes linear and well pad disturbances and excludes open-pit mines covering >25% of the area adjacent to and within wetlands. R, *p*-value (in brackets) and n observations are presented; bold indicates a significant relationship where alpha = 0.005.

| | Wetland characteristics | Change in shrub/tree area within wetlands | | Change in shrub/tree height | | Change in shrub/tree height standard deviation | |
|---|---|---|---|---|---|---|---|
| | | All HFI | Linear/wellpad HFI | All HFI | Linear/wellpad HFI | All HFI | Linear/wellpad HFI |
| Bog | L | −0.10 (0.11) | −0.09 (0.14) | −0.13 (0.05) | −0.14 (0.03) | 0.06 (0.38) | 0.03 (0.68) |
| $n$ = 246; 208 | A | −0.08 (0.20) | −0.08 (0.23) | −0.12 (0.06) | −0.14 (0.04) | 0.03 (0.68) | 0.06 (0.93) |
| | L:A | 0.09 (0.15) | 0.03 (0.64) | 0.03 (0.69) | 0.08 (0.22) | **−0.41 (<0.0001)** | **−0.24 (<0.0001)** |
| | %HFI | **0.19 (0.003)** | **0.28 (<0.0001)** | −0.09 (0.18) | −0.05 (0.42) | 0.04 (0.50) | 0.12 (0.07) |
| Fen | L | −0.02 (0.62) | −0.02 (0.61) | −0.05 (0.17) | −0.01 (0.80) | 0.04 (0.34) | 0.07 (0.09) |
| ($n$ = 738; 560) | A | −0.02 (0.65) | −0.02 (0.58) | −0.06 (0.12) | −0.01 (0.81) | 0.02 (0.62) | 0.05 (0.20) |
| | L:A | **−0.14 (0.0001)** | **−0.14 (0.0007)** | −0.07 (0.05) | −0.04 (0.40) | **−0.32 (<0.0001)** | **−0.38 (<0.0001)** |
| | %HFI | −0.03 (0.51) | −0.04 (0.32) | **−0.15 (<0.0001)** | **−0.16 (<0.0001)** | −0.05 (0.18) | −0.09 (0.03) |
| Marsh | L | 0.01 (0.85) | −0.05 (0.54) | −0.03 (0.67) | −0.05 (0.58) | 0.10 (0.18) | 0.08 (0.31) |
| ($n$ = 194; 146) | A | 0.006 (0.94) | −0.04 (0.63) | −0.07 (0.36) | −0.08 (0.36) | 0.05 (0.53) | 0.04 (0.64) |
| | L:A | −0.12 (0.11) | −0.06 (0.46) | −0.02 (0.83) | 0.04 (0.65) | **−0.49 (<0.0001)** | **−0.48 (<0.0001)** |
| | %HFI | −0.0002 (0.99) | 0.06 (0.47) | −0.06 (0.40) | −0.09 (0.27) | 0.03 (0.74) | 0.04 (0.67) |
| Swam | L | 0.03 (0.46) | 0.03 (0.44) | −0.03 (0.38) | −0.03 (0.33) | 0.07 (0.03) | 0.08 (0.04) |
| ($n$ = 802; 745) | A | 0.02 (0.66) | 0.02 (0.64) | −0.04 (0.33) | −0.04 (0.26) | 0.04 (0.24) | 0.04 (0.24) |
| | L:A | **−0.21 (<0.0001)** | **−0.22 (<0.0001)** | **−0.12 (0.001)** | **−0.16 (<0.0001)** | **−0.51 (<0.0001)** | **−0.51 (<0.0001)** |
| | %HFI | −0.04 (0.33) | **−0.14 (<0.0001)** | **−0.14 (<0.0001)** | **−0.18 (<0.0001)** | 0.05 (0.15) | 0.05 (0.15) |

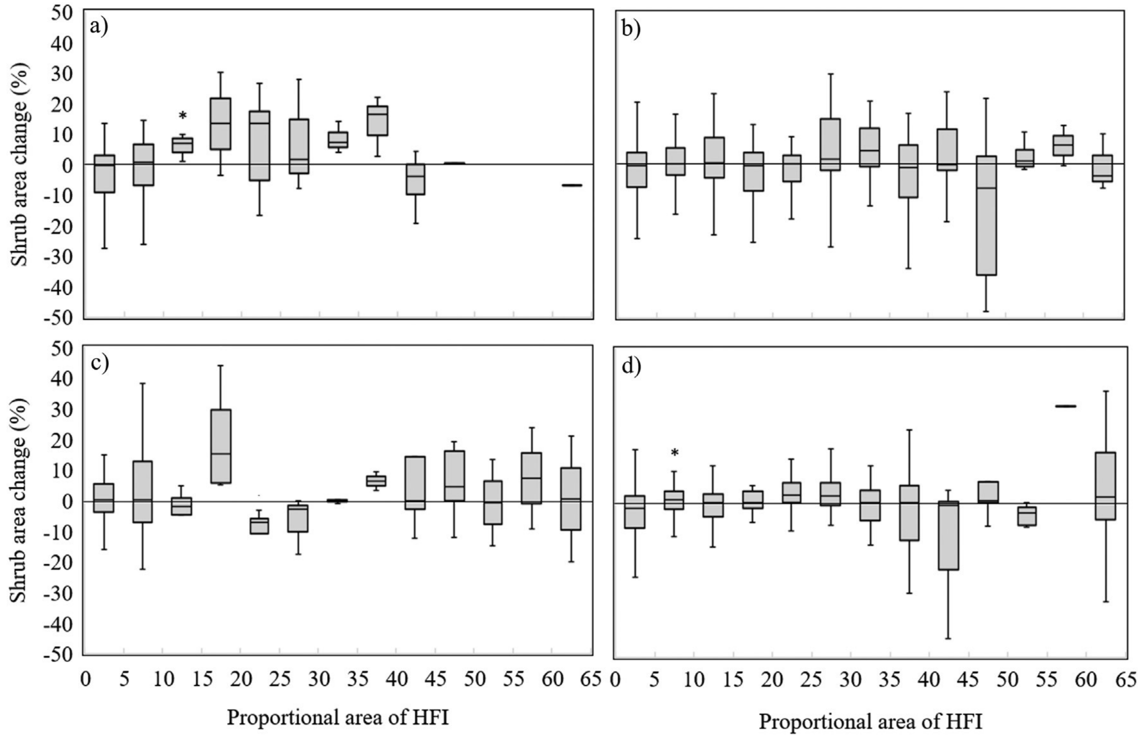


**Fig. 5.** Box plots for a) bog; b) fen; c) marsh; d) swamp showing mean, interquartile range, and 5th to 95th percentiles (whisker plots) change in wetland shrub and small tree proportional area from circa 2008 to 2018 (where positive change = increased area from 2008 to 2018) with increased proportional area of disturbance (% HFI). * represent significant differences (alpha = 0.01) from the mean in 2008, represented by zero found in undisturbed peatlands determined using a Bonferroni correction. Outliers are not shown in the figure because these would reduce the variability illustrated by the box plots, but are included in the statistical analysis.

be explored further, especially in areas undergoing rapid changes identified in Fig. 6.

Road and seismic line width and orientation across wetlands can also have influences on vegetation community changes by impact energy and water exchanges because they alter ground surface microtopography, and vegetation structural characteristics within and proximal to seismic lines (van Rensen et al., 2015; Abib et al., 2019). Similarly, the orientation of roads (Saraswati et al., 2020) and substrate type (Willier, 2017) can affect the degree of subsurface flow in wetlands, altering the movement of water, nutrients (Petrone et al., 2008) and gases, including release of methane gas (Moore and Dalva, 1993; Roulet et al., 1992). The proportion of anthropogenic disturbance can therefore influence wetland hydrologic functioning through changes to soil hydro-physical properties, compaction by direct placement of materials or infrastructure, which reduces peat bulk density and subsequently reduces subsurface flow, and water storage capacity, influencing the distribution and change of wetland vegetation through time (Volik et al., 2020).

### 4.3. Spatial variability of wetland vegetation height changes

We hypothesized that increased HFI proportion and fragmentation of wetlands could result changes in hydrology, which could enhance the growth of shrubs within wetlands between 2008 and 2018. We found that shrub and short tree heights between the two periods increased significantly with increased HFI disturbance in bogs ($R = 0.19$; $p = 0.003$). This relationship improved ($R = 0.28$, $p < 0.0001$) (Table 1) when large areas of open mine disturbances were excluded from the comparison (Table 1). The same relationship was not found in fens and swamps. In these wetlands, vegetation height declined between 2008 and 2018 with increased proportion of HFI, indicating that other complex environmental drivers may also be influencing vegetation change. Decline in shrub heights may be due to changes in groundwater discharge into fen and swamp wetlands, whereas isolated/ombrotrophic bogs typically receive little groundwater and therefore may be sensitive to the combined influences of HFI proportion and climatic drying observed during the period of study. However, these hypotheses require further testing, but correspond with some observations from the literature (Waddington et al., 2015). For example, Kettridge et al. (2013) found that decline in groundwater discharge to wetlands increased the sensitivity of some wetlands to drying, thereby increasing the propensity for further shrubification-drying feedbacks including increased transpiration and enhancement of shrub/tree density.

The length to area ratio of wetlands was also an important indicator of vegetation change between 2008 and 2018. While we expected that more complex shapes would yield greater density of shrubs, we found that fen and swamp wetlands with low length to area ratio (rounded shapes) experienced greater rates of shrub growth than elongated ones ($R = -0.14$ (fens), $-0.21$ (swamps); $p < 0.0001$) (Table 1). Also wetlands experienced a decline in shrub height variability with elongation. This was a surprising result as we expected that proximity to upland forests would enhance shrub growth due to greater proportion of ecotonal areas, though, L:A may be indicative of hydrological connectivity and resilience to drying (e.g. Thompson et al., 2019).

### 4.4. Implications for the future drivers: natural succession, disturbance and atmospheric deposition

Up to 30% of the proportional area of bogs along transects have experienced enhanced shrub and short tree growth over the last 10 years (Fig. 5). Changes in shrub growth and decline is likely influenced by local hydrology (Waddington et al., 2015), however, other influencing mechanisms not explored in this study may also influence vegetation change, including natural succession, climatic change/drying, local variations in hydrology, and atmospheric deposition from oil sands industry pollution. These may have important influences on the rates of change of vegetation communities in peatlands in this region, while,

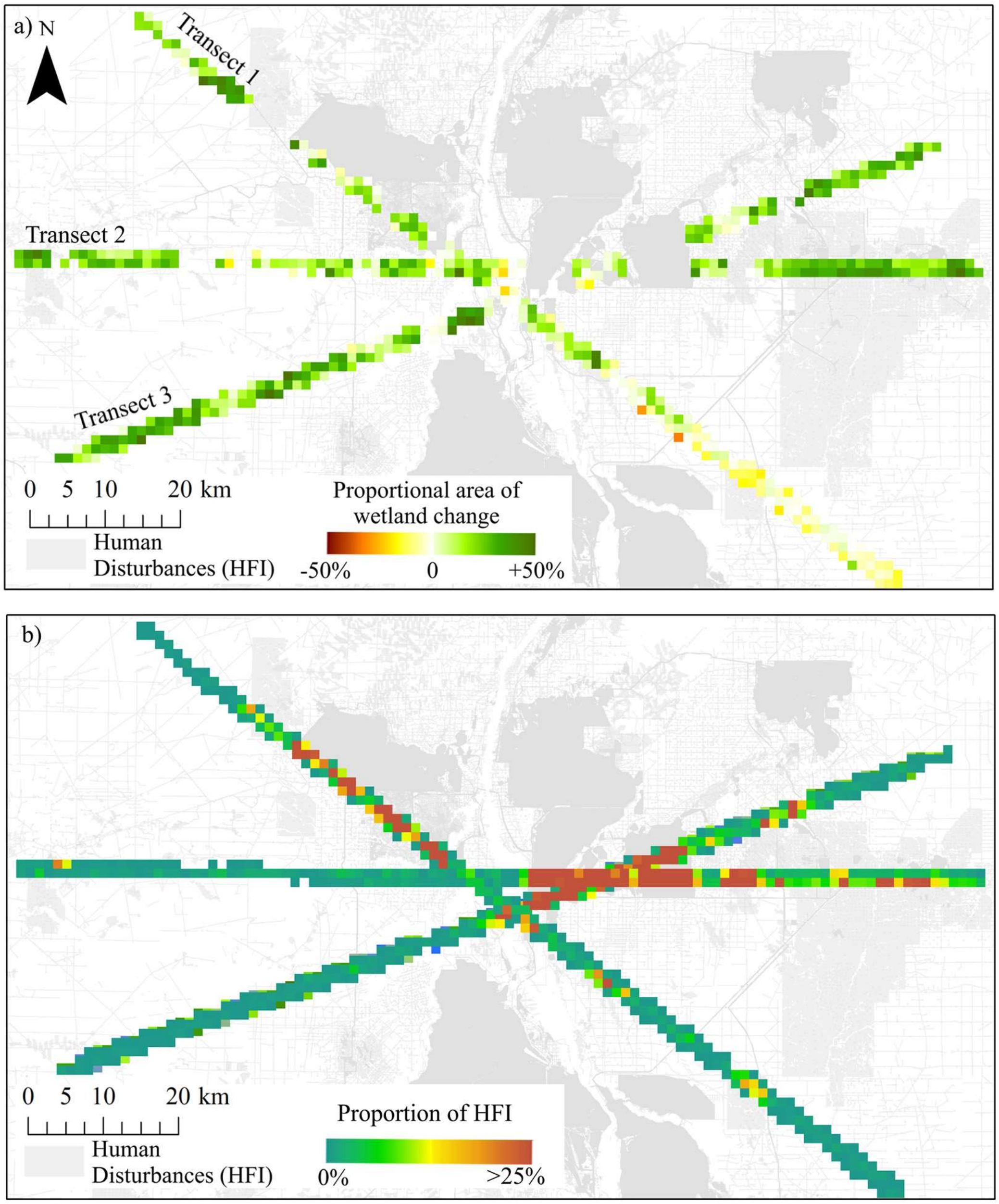


**Fig. 6.** a) Areas of cumulative proportional area of wetland change exceeding 1 m between 2008 and 2018, aggregated to 1 km grid cells calculated as the total area of both positive and negative changes in vegetation height over the ~10-year period. Missing cells represent areas that have open-pit mining; b) Density of HFI.

anthropogenic disturbances may have enhancing or mitigating influence when combined with these other driving mechanisms.

With regards to natural succession, the transition from open water marsh to fen (hydroseral succession) is the most frequently occurring autogenic succession in boreal peatlands (Charman, 2002; referred to in Kuhry and Turunen, 2006). This occurs as organic and mineral materials accumulate, transitioning open marshes into fens and then bogs. Accumulation of *Sphagnum* mosses make bogs increasingly rain-fed (ombrotrophic) over time, while also increasing their acidity, thereby impacting vegetation communities (Kuhry and Turunen, 2006). While some studies (e.g. Turunen et al., 2002) found that bogs accumulate peat faster than fens, causing them to become further upraised, Bauer et al. (2003) observed greatest rates of peat biomass accumulation within an area containing rich fen (though the area of the peatland complex is limited). As wetlands become drier, accumulation of peat declines (Kuhry, 1994) and conditions for shrubs such as *Salix* and *Betula* become more favorable (Bauer et al., 2003). Over longer periods (millennia), climatic changes can enhance rates of change, while groundwater discharge into fens (and resulting groundwater chemistry) can slow the transition of fens into bogs (Kubiw et al., 1989).

Anthropogenic disturbance can also alter the proximal wetland environment, potentially mimicking wet periods (peat depression and flooding) vs. dry periods (lowering water table) over a shortened time period. For example, lowering or simplifying of the ground surface elevation, which occurs during the development of seismic lines, can result in flooding in treed peatlands (Stevenson et al., 2019). Raising the ground in peatlands can increase drying and the growth of herbaceous vegetation, though responses can be complex and depends on peatland type and hydrological stability (Bauer et al., 2003). Stevenson et al. (2019) showed that local terrain complexity (e.g. micro hummocks and hollows) within seismic lines limited succession of trees and shrubs due to flooding. Abib et al. (2019) also found similar results within seismic lines, with reduced vegetation heights from centre to 15 m from seismic lines and increased vegetation height (determined from lidar) at distances of 15 m up to 50 m in peatlands. This occurred dominantly in peatlands disturbed by medium to wide seismic lines, those that had south and west-facing edges, and older seismic line disturbances. Using a random forest regression-tree analysis, Abib et al. (2019) found that distance, width, cardinal direction, and topographic position were among the greatest influences on the growth of shrubs within peatlands, illustrating the complexity of influences that variations in the development of these particular disturbances could have on peatlands. In this study, we find that bogs impacted by greater proportional area disturbances experience increases in shrub height and succession, while the influence of disturbance on fens, marshes and swamps is less clear. Future research should examine variation in peat accumulation and topographic variability adjacent to different disturbances to better understand connections between elevation, depth to water table, and shrub/tree succession within different wetland classes. For example, it could be hypothesized that seismic line depression of bogs combined with greater depth to water table and increased tension compared with fens may result in groundwater movement into seismic lines and further evaporative losses, while areas proximal to seismic lines could remain topographically upraised. A second hypothesis could be developed for fen elevation, where near surface water table combined with local depression from seismic lines may depress the area of peat within and proximal to seismic lines associated with flooding and plastic deformation of peat and saturated pore water spaces.

Several studies have also examined the influence of interpolated atmospheric deposition on vegetation successional processes and accumulation of biomass within the OSR. Wieder et al. (2019) hypothesized that nitrogen (N) deposition may have a significant impact, especially on ombrotrophic bogs in this region, where atmospheric N emissions can be as high as 17 kg $N \cdot ha^{-1} \cdot yr^{-1}$, while regional deposition is typically <2 kg $N \cdot ha^{-1} \cdot yr^{-1}$. The concentration of deposition has been found to vary with distance from the mining sites (Edgerton et al., 2020). Using atmospheric deposition concentrations supported by Edgerton et al. (2020), Bartels et al. (2019) found that biomass in highly sensitive jack pine and understory forests in relatively dry uplands increased in areas that received greater deposition of N and S. Shrub proportional coverage within jack pine stands was also positively related to both increased S deposition as well as potential acid input, which created a fertilization effect. In wetland ecosystems, using experimental application of N on an OSR bog, Wieder et al. (2019) found that vascular and shrub species including *Picea mariana* and other ericaceous shrubs increased in rate of growth with higher concentrations of N deposition, while growth of *Sphagnum fuscum* was inhibited. Edgerton et al. (2020) found mean N loading at sites near oil sands mines was ~1.2 to 5 kg-$N \cdot ha^{-1} \cdot yr^{-1}$, which is slightly elevated from the regional deposition estimates described in Wieder et al. (2010, 2019) and are lower than experimental applications associated with enhanced vegetation growth. Earlier research by Wieder et al. (2010) found no significant influences of regional atmospheric concentrations of N or S on natural *Sphagnum fuscum* productivity with distance from mines. Further, Wieder et al. (2016) note the complicating influences of late summer precipitation and increased aridity influences on ombrotrophic bog *Sphagnum fuscum* growth. Bi-temporal lidar data of vegetation changes, anthropogenic disturbance, hydrological drivers may allow for improved separability of these drivers along with interpolated atmospheric concentrations of N and S deposition in the future due the numbers of bogs and spatial variations in terrain, vegetation growth, shape, disturbance and other influencing factors.

### 4.5. Recommendations

This study illustrates that shrub and short tree changes in height can be identified across hundreds of wetlands in the OSR using bi-temporal lidar data. These datasets provide an opportunity to examine the relationships between vegetation growth, wetland characteristics, such as shape complexity, and the proportional coverage of HFI. We found that, the relationships between wetland shrub development, fragmentation due to anthropogenic disturbances and proportion of HFI are complex, varying between wetland classes and disturbance proportions. Transect 3 (Fig. 4) demonstrated a significant relationship between HFI density and increasing wetland complexity, and while we also observed a similar pattern in Transect 2, the relationship was less clear in areas with greater proportional coverage of HFI associated with open mine sites. We also found that bogs were most susceptible to increased shrubification, while we observed a net decline in height and area of shrubs and short trees in fens and swamps, and as these became more elongated (Table 1, Fig. 5).

We recommend that future analyses examine why these broad, complex generalizations found in this study exist. Lidar data provide the opportunity to examine how local environmental drivers may be influencing growth or decline of vegetation. Each interpolated grid cell, therefore, represents a measurement of change, which could then be related to other attributes of the local environment within the thematic lidar-based derivations. These may include local topographic influences derived from ground surface elevation, which may be related to the nearness of the ground surface to the water table, proximal ecotonal and upland forests, and estimates of energy balance associated with shading of surrounding trees, among other attributes (e.g. slope, aspect, shape, etc.). Changes in vegetation height and extent should also be related to the type and shape of disturbance (e.g. open mining, forest harvest) and in the case of seismic lines, their various characteristics (e.g. Abib et al., 2019) including width, orientation and age, and also wetland form (treed, shrub, gramminoid). In addition to these, changes in the concentration of atmospheric deposition with distance from mining operations could also be examined.

As wetlands become increasingly fragmented, shrub growth especially within bogs, could make these peatlands more sensitive to drying, enhancing further fragmentation (Waddington et al., 2015; Thompson et al., 2019). The potential to quantify changes across hundreds of wetlands provides an opportunity to control for the influence of hydrology and other attributes of the land surface beyond what could be measured in the field, alone. Lidar provides a relatively inexpensive extension of field data collection of vegetation structure (Chasmer et al., 2020b). Further, the use of bi-temporal lidar data allows us to determine the driving mechanisms that result in fragmentation and those that retain regional wetland characteristics, which are important understanding the cumulative impacts of these, climate-mediated stressors (Stralberg et al., 2020), the implications to ecosystem services, and where ecosystem management strategies should be considered (Fig. 6).

## 5. Conclusions

In this study, we used a unique, relatively low-cost bi-temporal lidar-based sampling method to quantify spatial variations in wetland vegetation structure and change through time. Using the lidar-based approach, we have identified areas of significant but complex vegetation change within wetlands of the OSR. In addition, lidar provides an effective approach for identifying changes in wetland vegetation and could be used as a method for future monitoring and assessment. Here we found that wetland complexity is greater in areas with high proportions of linear disturbances such as seismic lines, roads, and oil pipelines but this relationship declines with greater proportional coverage of large open mine areas. This increased the propensity for changes in height and expansion of shrubs and trees, especially in bogs, while decline of height was observed in fens and swamps in general, though the relationships are complex. We suggest that increased wetland complexity may enhance climate-mediated disturbances, but these complex relationships need to be quantified. Therefore, further research is required to elucidate the more complex drivers of local wetland vegetation community change. We also recommend further monitoring, especially in areas of rapid change identified in this study by using an integrated field survey and remote sensing approach that provides a regional assessment of wetland ecosystem health indicators.

## CRediT authorship contribution statement

LC and DC proposal for research and funding; CH lidar data collection and initial processing; LC, EML, CM writing and analysis; CM, EML, JM data processing; LC, CH, DC, CM, EML manuscript ideas, conceptualization; LC, EML, CM, CH, JM, DC, document editing.

## Funding

Funding was provided by the Government of Alberta under the Oil Sands Monitoring Program (18GRAEM24-01).

## Availability of data and material

Data are available through licensing and data agreements with the Government of Alberta.

## Code availability

Not applicable.

## Declaration of competing interest

Not applicable.

## Acknowledgements

This research was funded by Government of Alberta under the Oil Sands Monitoring Program (18GRAEM24-01) to Drs. Danielle Cobbaert and Laura Chasmer. Ph.D. candidate Mr. Moura Lima was supported by the Emerging Leaders of the Americas internship program at the University of Lethbridge. We would also like to acknowledge the important assistance of Mr. Maxim Okhrimenko, University of Lethbridge, for Titan MS lidar data collection and processing. Thank-you to three anonymous reviewers who provide excellent suggestions to improve our manuscript. The authors declare that there are no conflicts of interest.

## References

Abib, T.H., Chasmer, L., Hopkinson, C., Mahoney, C., Rodriguez, L.C.E., 2019. Seismic line impacts on proximal boreal forest and wetland environments in Alberta. Sci. Total Environ. 658, 1601–1613.

ABMI, 2016. 3 × 7 Photoplot Land Cover Dataset Data Model, Version 2.4.1. Alberta Biodiversity Monitoring Institute Available at:. https://ftp-public.abmi.ca//GISData/HumanFootprint3x7PhotoPlotLandCover/ABMI_photoplot_DataModel_v241_20160212.pdf. (Accessed May 2020).

ABMI, 2019. ALPHA Program, Predictive Landcover (PLC) 3.0 and ABMI Wetland Inventory – metadata. Alberta Biodiversity Monitoring Institute Available at:. https://ftp-public.abmi.ca//GISData/PredictiveLandcover/PLC30_OS_metadata.pdf. (Accessed May 2020).

ABMI Human Footprint Inventory, 2019. Wall-to-Wall Human Footprint Inventory. Alberta Biodiversity Monitoring Institute and Alberta Human Footprint Monitoring Program. ABMI - Wall-to-Wall Human Footprint Inventory, Edmonton, AB.

Alberta Energy Regulator, 2019. ST98: Alberta Energy Outlook. Alberta Energy Regulator. Available at:. https://www.aer.ca/providing-information/data-and-reports/statistical-reports/st98.html. (Accessed May 2020).

Atkinson, N., Utting, D.J., Pawley, S.M., 2014. Glacial Landforms of Alberta, Canada. Available at:. https://ags.aer.ca/publications/MAP_604.html. (Accessed May 2020).

Bartels, S.F., Gendreau-Berthiaume, B., Macdonald, S.E., 2019. The impact of atmospheric acid deposition on tree growth and forest understory vegetation in the Athabasca Oil Sands Region. Sci. Total Environ. 696, 133877.

Bauer, I.E., Gignac, L.D., Vitt, D.H., 2003. Development of a peatland complex in boreal western Canada: lateral site expansion and local variability in vegetation succession and long-term peat accumulation. Can. J. Bot. 81, 833–847.

Charman, D.J., 2002. Peatlands and Environmental Change. John Wiley and Sons, Ltd (301 pgs.).

Chasmer, L., Hopkinson, C., Petrone, R., Devito, K., 2018. Remote sensing of ecosystem trajectories as a proxy-indicator for watershed water balance. Ecohydrology. E1987. https://doi.org/10.1002/eco.1987.

Chasmer, L., Cobbaert, D., Millard, K., Peters, D.L., Devito, K., Brisco, B., Hopkinson, C., Mahoney, C., Merchant, M., Montgomery, J., Nelson, K., Niemann, O., 2020a. Remote sensing of boreal wetlands 1: data use for policy and management. Remote Sensing: Special Issue on Wetland Change 12, 1320. https://doi.org/10.3390/rs12081320.

Chasmer, L.D., Mahoney, C., Millard, K., Nelson, K., Peters, D., Merchant, M., Hopkinson, C., Brisco, B., Niemann, O., Montgomery, J., Devito, K., Cobbaert, D., 2020b. Remote sensing of boreal wetlands 2: methods for evaluating boreal wetland ecosystem state and drivers of change. Remote Sens. Spec. Issue Wetl. Change 12, 1321.

Dabros, A., Pyper, M., Castilla, G., 2018. Seismic lines in the boreal and arctic ecosystems of North America: environmental impacts, challenges, and opportunities. Environ. Rev. 26, 214–229.

DeLancey, E.R., Kariyeva, J., Bried, J.T., Hird, J.N., 2019. Large-scale probabilistic identification of boreal peatlands using Google Earth Engine, open-access satellite data, and machine learning. PLoS One 14, e0218165.

Devito, K., Creed, I., Gan, T., Mendoza, C., Petrone, R., Silins, U., Smerdon, B., 2005. A framework for broad-scale classification of hydrologic response units on the boreal plain: is topography the last thing to consider? Hydrol. Process. 19, 1705–1714.

Devito, K., Mendoza, C., Qualizza, C., 2012. Conceptualizing water movement in the boreal plains. Implications for Watershed Reconstruction. Environmental and Reclamation Research Group Synthesis report prepared for the Canadian Oil Sands Network for Research and Development. (165 pp.).

ECCC, 2019. Canadian Climate Normals - Fort McMurray A. Environment and Climate Change Canada. Available at:. https://climate.weather.gc.ca/climate_normals/index_e.html. (Accessed December 2019).

Edgerton, E.S., Hsu, Y.-M., White, E.M., Fenn, M.E., Landis, M.S., 2020. Ambient concentrations and total deposition of inorganic sulfur, inorganic nitrogen and base cations in the Athabasca Oil Sands Region. Sci. Total Environ. 706, 134864.

ESRD, 2015. Alberta Wetland Classification System. Alberta Environment and Sustainable Resource Development. Available at:. https://open.alberta.ca/dataset/92fbfbf5-62e1-49c7-aa13-8970a099f97d/resource/1e4372ca-b99c-4990-b4f5-dbac23424e3a/download/2015-Alberta-Wetland-Classification-System-June-01-2015.pdf. (Accessed May 2020).

Fenton, M.M., Waters, E.J., Pawley, S.M., Atkinson, N., Utting, D.J., McKay, K., 2013. Surficial geology of Alberta. Alberta Geological Survey, AER/AGS Map. 601.

Ficken, C.D., Cobbaert, D., Rooney, R.C., 2019. Low extent but high impact of human land use on wetland flora across the boreal oil sands region. Sci. Total Environ. 693, 133647.

Finnegan, L., MacNearney, D., Pigeon, K.E., 2018. Divergent patterns of understory forage growth after seismic line exploration: implications for caribou habitat restoration. For. Ecol. Manag. 409, 634–652.

Flannigan, M.D., Wotton, B.M., Marshall, G.A., de Groot, W.J., Johnston, J., Jurko, N., Cantin, A.S., 2015. Fuel moisture sensitivity to temperature and precipitation: climate change implications. Clim. Chang. 134, 59–71.

Goodale, R., Hopkinson, C., Colville, D., Amirault, D., 2007. Mapping piping plover habitat in coastal areas using airborne lidar data. Can. J. Remote. Sens. 33 (6), 519–533.

Groot, A., Carlson, D.W., Fleming, R.L., Wood, J.E., 1997. Small openings in trembling aspen forest: microclimate and regeneration of white spruce and trembling aspen. NODA/NFP Technical Report TR-47 31 pgs. (ISBN 0-662-25461-9).

Hesselbarth, M.H.K., Sciaini, M., With, K.A., Wiegand, K., Nowosad, J., 2019. Landscapemetrics: an open-source R tool to calculate landscape metrics. Ecography 42, 1648–1657.

Hokanson, K.J., Mendoza, C.A., Devito, K.J., 2019. Interactions between regional climate, surficial geology, and topography: characterizing shallow groundwater systems in subhumid, low-relief landscapes. Water Resour. Res. 55 (1), 284–297.

Hokanson, K.J., Peterson, E.S., Devito, K.J., Mendoza, C.A., 2020. Forestland-peatland hydrologic connectivity in water-limited environments: hydraulic gradients often oppose topography. Environ. Res. Lett. 15 (3), 034021.

Hopkinson, C., Chasmer, L., Hall, R.J., 2008. The uncertainty in conifer plantation growth prediction from multi-temporal lidar datasets. Remote Sens. Environ. 112 (3), 1168–1180. https://doi.org/10.1016/j.rse.2007.07.020.

Hopkinson, C.L., Chasmer, L., Barr, A.G., Kljun, N., Black, T.A., McCaughey, J.H., 2016a. Monitoring boreal forest biomass and carbon storage change by integrating airborne laser scanning, biometry and eddy covariance data. Remote Sens. Environ. 181, 82–95.

Hopkinson, C., Chasmer, L., Gynan, C., Mahoney, C., Sitar, M., 2016b. Multisensor and multispectral lidar characterization and classification of a forest environment. Can. J. Remote. Sens. 42 (5), 501–520.

IPCC, 2014. Climate change 2014: synthesis report. Contribution of Working Groups I, II and III to the Fifth Assessment Report of the Intergovernmental Panel on Climate Change (Geneva, Switzerland. 151 pp.).

Ireson, A.M., Barr, A.G., Johnstone, J.F., Mamet, S.D., van der Kamp, G., Whitfield, C.J., Michel, N.L., North, R.L., Westbrook, C.J., DeBeer, C., Chun, K.P., Nazemi, A., Sagin, J., 2015. The changing water cycle: the Boreal Plains ecozone of Western Canada. Wiley Interdiscip. Rev. Water 2, 505–521.

Jiang, R., Gan, T.Y., Xie, J., Wang, N., Kuo, C.-C., 2015. Historical and potential changes of precipitation and temperature of Alberta subjected to climate change impact: 1900–2100. Theor. Appl. Climatol. 127, 725–739.

Ketcheson, S.J., Price, J.S., Carey, S.K., Petrone, R.M., Mendoza, C.A., Devito, K.J., 2016. Constructing fen peatlands in post-mining oil sands landscapes: challenges and opportunities from a hydrological perspective. Earth Sci. Rev. 161, 130–139.

Kettridge, N., Thompson, D.K., Bombonato, L., Turetsky, M.R., Benscoter, B.W., Waddington, J.M., 2013. The ecohydrology of forested peatlands: simulating the effects of tree shading on moss evaporation and species composition. J. Geophys. Res. Biogeosci. 118 (2), 422–435.

Kubiw, H., Hickman, M., Vitt, D.H., 1989. The developmental history of peatlands at Muskiki and Marguerite Lakes, Alberta (Canada). Can. J. Bot. 67, 3534–3544.

Kuhry, P., 1994. The role of fire in the development of Sphagnum-dominated peatlands in western boreal Canada. J. Ecol. 82, 899–910.
Kuhry, P., Turunen, J., 2006. The postglacial development of boreal and sub-arctic peatlands. In: Wieder, R.K., Vitt, D.H. (Eds.), Boreal Peatland Ecosystems. Springer-Verlag, pp. 25–45.
Lee, P., Boutin, S., 2006. Persistence and developmental transition of wide seismic lines in the western Boreal Plains of Canada. J. Environ. Manag. 78, 240–250.
Lefsky, M.A., Cohen, W.B., Acker, S.A., Parker, G.G., Spies, T.A., Harding, D., 1999. Lidar remote sensing of the canopy structure and biophysical properties of Douglas-fir western hemlock forests. Remote Sens. Environ. 70, 339–361.
Lovitt, J., Rahman, M.M., Saraswati, S., McDermid, G.J., Strack, M., Xu, B., 2018. UAV remote sensing can reveal the effects of low-impact seismic lines on surface morphology, hydrology, and methane (CH4) release in a boreal treed bog. J. Geophys. Res. Biogeosci. 123, 1117–1129.
MacCormack, K.E., Atkinson, N., Lyster, S., 2015. Sediment thickness of Alberta. Alberta Geological Survey, AER/AGS Map. 603.
Mahoney, C., Hall, R.J., Hopkinson, C., Filiatrault, M., Beaudoin, A., Chen, Q., 2018. A forest attribute mapping framework: a pilot study in a Northern Boreal Forest, Northwest Territories, Canada. Remote Sens. 10, 1338.
Montgomery, J., Brisco, B., Chasmer, L., Devito, K., Cobbaert, D., Hopkinson, C., 2019. SAR and Lidar temporal data fusion approaches to boreal wetland ecosystem monitoring. Remote Sens. 11, 161.
Moore, T.R., Dalva, M., 1993. The influence of temperature and water table position on carbon dioxide and methane emissions from laboratory columns of peatland soils. J. Soil Sci. 44 (4), 651–664. https://doi.org/10.1111/j.1365-2389.1993.tb02330.x.
Mwale, D., Gan, T.Y., Devito, K., Mendoza, C., Silins, U., Petrone, R., 2009. Precipitation variability and its relationship to hydrologic variability in Alberta. Hydrol. Process. 23, 3040–3056.
Nwaishi, F., Petrone, R.M., Price, J.S., Andersen, R., 2015. Towards developing a functional-based approach for constructed peatlands evaluation in the Alberta Oil Sands Region, Canada. Wetlands 35, 211–225.
Petrone, R.M., Silins, U., Devito, K.J., 2007. Dynamics of evapotranspiration from a riparian pond complex in the Western Boreal Forest, Alberta, Canada. Hydrol. Process. 21, 1391–1401.
Petrone, R.M., Devito, K.J., Silins, U., Mendoza, C., Brown, S.C., Kaufman, S.C., Price, J.S., 2008. Transient peat properties in two pond-peatland complexes in the sub-humid Western Boreal Plain, Canada. Mires & Peat 3, 1–13.
Petrone, R.M., Chasmer, L., Hopkinson, C., Silins, U., Landhäusser, S.M., Kljun, N., Devito, K.J., 2015. Effects of harvesting and drought on $CO_2$ and $H_2O$ fluxes in an aspen-dominated western boreal plain forest: early chronosequence recovery. Can. J. For. Res. 45, 87–100.
van Rensen, C.K., Nielsen, S.E., White, B., Vinge, T., Lieffers, V.J., 2015. Natural regeneration of forest vegetation on legacy seismic lines in boreal habitats in Alberta's oil sands region. Biol. Conserv. 184, 127–135.
Revel, R.D., Dougherty, T.D., Downing, D.J., 1984. Forest Growth and Revegetation Along Seismic Lines. University of Calgary Press, Calgary, Alberta, Canada.
Rooney, R.C., Bayley, S.E., Schindler, D.W., 2012. Oil sands mining and reclamation cause massive loss of peatland and stored carbon. Proc. Natl. Acad. Sci. 109, 4933–4937.
Roulet, N., Moore, T.I.M., Bubier, J., Lafleur, P., 1992. Northern fens: methane flux and climatic change. Tellus B 44 (2), 100–105. https://doi.org/10.1034/j.1600-0889.1992.t01-1-00002.x.
Saraswati, S., Petrone, R.M., Rahman, M.M., McDermid, G.J., Xu, B., Strack, M., 2020. Hydrological effects of resource-access road crossings on boreal forested peatlands. J. Hydrol. 584, 124748.
Smerdon, B.D., Mendoza, C.A., Devito, K.J., 2008. Influence of subhumid climate and water table depth on groundwater recharge in shallow outwash aquifers. Water Resour. Res. 44, W08427.
Stevenson, C., Filicetti, A., Nielsen, S., 2019. High precision altimeter demonstrates simplification and depression of microtopography on seismic lines in treed peatlands. Forests 10, 295.
Stralberg, D., Arsenault, D., Baltzer, J., et al., 2020. Climate-change refugia in boreal North America: what, where, and for how long? Front. Ecol. Environ. 18 (5), 261–270.
Thompson, C., Mendoza, C.A., Devito, K.J., 2017. Potential influence of climate change on ecosystems within the Boreal Plains of Alberta. Hydrol. Process. 31, 2110–2124.
Thompson, D.K., Simpson, B.N., Whitman, E., Barber, Q.E., Parisien, M.A., 2019. Peatland hydrological dynamics as a driver of landscape connectivity and fire activity in the boreal plain of Canada. Forests 10 (7), 534.
Turunen, J., Tomppo, E., Tolonen, K., Reinikainen, A., 2002. Estimating carbon accumulation rates of undrained mires in Finland: application to boreal and subaractic regions. The Holocene 12, 69–80.
Volik, O., Elmes, M., Petrone, R., Kessel, E., Green, A., Cobbaert, D., Price, J., 2020. Wetlands in the Athabasca Oil Sands Region: the nexus between wetland hydrological function and resource extraction. Environ. Rev., 1–16 https://doi.org/10.1139/er-2019-0040.
Waddington, J.M., Morris, P.J., Kettridge, N., Granath, G., Thompson, D.K., Moore, P.A., 2015. Hydrological feedbacks in northern peatlands. Ecohydrology 8 (1), 113–127. https://doi.org/10.1002/eco.1493.
Walker, X.J., Rogers, B.M., Veraverbeke, S., et al., 2020. Fuel availability not fire weather controls boreal wildfire severity and carbon emissions. Nat. Clim. Chang. https://doi.org/10.1038/s41558-020-00920-8.
Wieder, R.K., Vitt, D.H., Burke-Scoll, M., Scott, K.D., House, M., Vile, M.A., 2010. Nitrogen and sulfur deposition and the growth of Sphagnum fuscum in bogs of the Athabasca Oil Sands Region. J. Limnol. 69 (Suppl.1), 161–170.
Wieder, R.K., Vile, M.A., Scott, K.D., Albright, C.M., McMillen, K.J., Vitt, D.H., Fenn, M.E., 2016. Differential effects of high atmospheric N and S deposition on bog plant/lichen tissue and porewater chemistry across the Athabasca Oil Sands Region. Environ. Sci. Technol. 50, 12630–12640.
Wieder, R.K., Vitt, D.H., Vile, M.A., Graham, J.A., Hartsock, J.A., Fillingim, H., House, M., Quinn, J.C., Scott, K.D., Petix, M., McMillen, K.J., 2019. Experimental nitrogen addition alters structure and function of a boreal bog: critical load and thresholds revealed. Ecol. Monogr. 89, e01371.
Willier, C.N., 2017. Changes in Peatland Plant Community Composition and Stand Structure Due to Road Induced Flooding and Desiccation. ERA Fall 2017.
Wulder, M.A., White, J.C., Bater, C.W., Coops, N.C., Hopkinson, C., Chen, G., 2012. Lidar plots—a new large-area data collection option: context, concepts, and case study. Can. J. Remote. Sens. 38 (5), 600–618.